Directionality of the ambient noise field in an Arctic, glacial bay

Grant B. Deane
Scripps Institution of Oceanography, University of California–San Diego, San Diego, California 92093-0206
gdeane@ucsd.edu

Oskar Glowacki
Institute of Geophysics, Polish Academy of Sciences, Warsaw, Poland
oglowacki@igf.edu.pl

Jaroslaw Tegowski
Institute of Oceanography, University of Gdansk, Gdansk, Poland
j.tegowski@ug.edu.pl

Mateusz Moskalik
Institute of Geophysics, Polish Academy of Sciences, Warsaw, Poland
mmosk@igf.edu.pl

Philippe Blondel
University of Bath, Bath, United Kingdom
pyspb@bath.ac.uk

Abstract: The directionality of ambient noise in an Arctic tidewater glacier bay was measured using two horizontally spaced, broadband hydrophones. Segments of noise were divided into two frequency bands and analyzed for arrival angle. These data show that different classes of source radiate noise in distinct spectral bands and are spatially diverse. A previously unidentified source, the interaction of surface gravity waves with underside of ice ledges at the periphery of icebergs, is described. The generation of noise by ice-wave interaction suggests that surface waves should be measured if ambient noise is to be used to monitor ice dynamics in glacial fjords.

PACS numbers: 43.30.Nb, 43.30.Pc [JL]
Date Received: July 20, 2014 **Date Accepted:** September 16, 2014

1. Introduction

The study of underwater ambient noise in the Arctic extends back to the 1960s, with early results presented by Macpherson (1962), Greene and Buck (1964), and Milne and Ganton (1964). Much of the work since then has been concerned with the generation, propagation, and statistical properties of noise generated by sea ice, consistent with the observation that the interaction of the ice cover with the air and water boundary layer is the primary source of noise production (Carey and Evans, 2011). More recently, interest has extended to the underwater noise in Arctic fjords, particularly those that contain glaciers and freshwater ice.

Ocean-ice boundaries in both the Arctic and Antarctic are dynamic regions that are gaining increasing attention as sensitive indicators of shifts in climate. The application of ambient noise oceanography in these fjords offers an opportunity to study the dynamics of marine-terminating glaciers in the Arctic. There are already many useful and well-established measurement systems for studying glaciers and glacier dynamics, including satellite imagery, GPS, seismometers, ice penetrating radar, and so on. However, ambient noise oceanography—the use of naturally generated underwater acoustic signals to study source mechanisms and the environment through which the noise propagates—presents some attractive advantages. Sound can propagate long distances underwater and systems to monitor underwater ambient noise for up to a year or more are readily available, relatively inexpensive, and easy to deploy.

The main difficulty in using the noise in the vicinity of marine-terminating glaciers is not so much in the measurements as it is in understanding their significance. Quantitative monitoring of glacier dynamics through underwater sound depends upon knowledge of the mechanisms producing the sound and their relationship to source spectrum and generation statistics.

Pettit *et al.* (2012) have reported three distinct physical processes contributing to the ambient noise field in tidewater glacial fjords; namely, iceberg calving, ice melt, and freshwater discharge. Glacial ice typically contains air bubbles, entrained when the ice is first formed out of snow and slowly compacted and pressurized as overburden pressure increases over time. The pressure inside gas bubbles within Arctic glacier ice can reach 2 MPa (Scholander and Nott, 1960), so the release of gas as the ice melts can be a noisy process. It is referred to as "Seltzer ice" by submariners (Wadhams, personal communication) and Urick (1971) appears to have published the first measurements of noise from melting glacier ice, and attributed the sound produced to "…the explosion of tiny air bubbles entrapped in the ice under pressure and released as melting occurs." Iceberg calving is accompanied by the entrainment of significant quantities of air, which is a noisy process, and may also excite low-frequency acoustic emissions through the face of the glacier. In a preliminary interpretation, Pettit *et al.* (2012) attribute their observations of diurnal variations in the sound pressure level of low-frequency sound in the range 90–110 Hz in Icy Bay, Alaska to freshwater discharge, possibly through the mechanisms of low-frequency sound emission associated with water resonance in cracks and cavities. Here we propose a fourth mechanism, which is ice-wave interactions radiating sound in the approximate band 100–500 Hz.

Single-hydrophone measurements by Keogh and Blondel (2008), made in summer 2007 along Kongsfjord in Svalbard, clearly distinguished the higher-frequency acoustic signatures of small icebergs from other environmental processes. Tegowski *et al.* (2011) made broadband, single-hydrophone measurements of the ambient noise in two fjords during the summer of 2009 in Svalbard. The fjords differed significantly in their surrounding environment: the Hornsund fjord, surrounded by mountains and melting glaciers, and the Murchison fjord, which is devoid of glaciers but full of floating ice floes. Measurements in the frequency band 20 Hz–24 kHz were made with an omnidirectional International Transducer Corporation (ITC) 6050C hydrophone, deployed 18 m below the surface. A statistical analysis of the noise demonstrated that the probability density distribution of noise in the spectral band (20–1000) Hz was not normally distributed, and suggestive of the presence of a few, loud sources, whereas the noise above 2.5 kHz was normally distributed and consistent with a large number of distributed and superposed sources (Tegowski *et al.*, 2012).

Here we present measurements of the ambient noise made in Hornsund fjord during the summer of 2013. Building on the earlier study by Tegowski *et al.* (2011), the objective of this field campaign was to see if low-frequency (20–3000) Hz and high-frequency (3–20) kHz noise within the fjord could be unequivocally associated with distinct and separate sources.

2. Experiment description

Noise recordings were made around Hans glacier in Hornsund fjord located on southwestern Spitsbergen, Svalbard. A satellite photograph of the glacier and its foreground is shown in Fig. 1. Colors within the fjord indicate water depth and a length scale is given on the bottom right. The photographs on the top left and right, respectively, show the recording system (described below) and the glacier terminus viewed from the western bluff. There were nine measurement sites studied over three days labeled

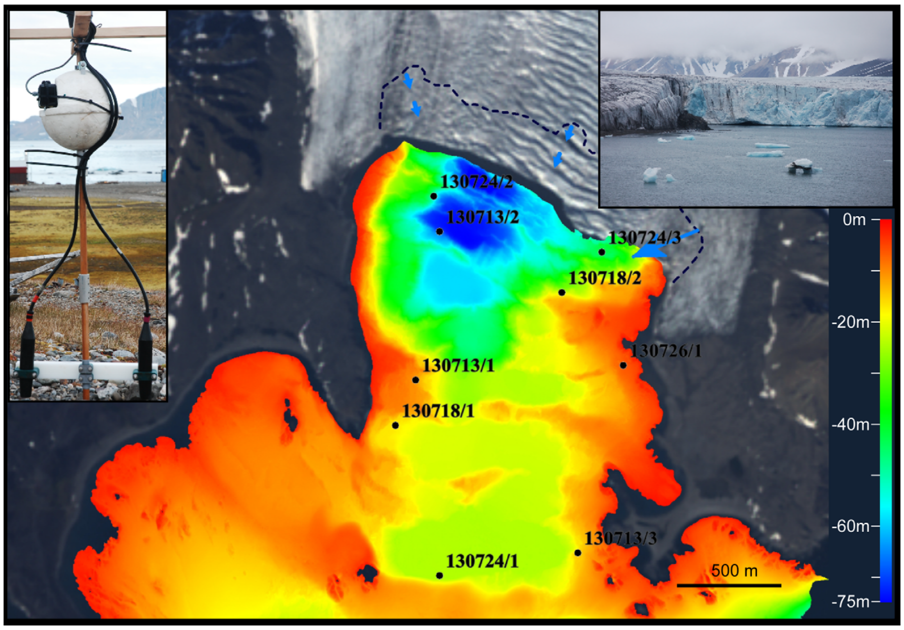

FIG. 1. (Color online) A satellite image of Hans glacier (AlosAvnir 2009.07.11) with bathymetry (depth data from The Norwegian Hydrographic Service with permit number 13/G722) superimposed in COLORGLOW. Upper left: A photograph of the two-element directional acoustic array (DAB). Upper right: A photograph of the glacier wall taken from the western bluff. Recording sites are designated with yymmdd/j where yy = 13, mm = 07, dd = 18, 24, and 26, and j = 1,2,3. Black line—the position of the glacier terminus on 2014.08.24, blue arrows show the locations of subglacial freshwater outflows.

1307dd/j where dd = 13, 18, and 24 corresponds to the survey day in July 2013 ("1307") and j = 1, 2, and 3 enumerates the sites within the day. The black line indicates the position of the glacier terminus, relative to the slightly older satellite image, and the blue arrows indicate the locations of subglacial freshwater outflows.

Ambient noise measurements were made with the purpose-built directional acoustic buoy (DAB) consisting of two ITC 6050C hydrophones mounted 0.43 m apart on a horizontal bar and connected to a surface float by a 1-m long vertical support. DAB records ambient noise with a Sony TCD-D8 digital tape recorder while a GPS, a magnetic compass and two tilt sensors housed in a splash-proof Pelican case provide array position, heading and tilt. The compass works well under calm ocean conditions, but the strong magnetic inclination (82°) at Svalbard's latitude caused problems for the instrument if its tilt from the horizontal exceeded approximately 5°. For this reason, DAB was modified part way through the deployment by adding crossed spars and a ship's compass to the top, to provide control and visual confirmation of its heading. Ambient noise recordings of 20–30 min were preceded with a 1-min segment of white noise of known spectral level to provide a system calibration. Photographs and/or videos of the surrounding geographical location were taken, along with notes of any factors of particular interest, such as the presence of ships or icebergs.

The geometry for the array processing scheme shown in Fig. A1 of Deane (1999). An acoustic arrival is shown incident at an angle θ to the array axis. The hydrophones are separated by a distance $L = 0.43$ m. For the following analysis we have chosen the frequency ranges 20–3000 Hz and 3000–20 000 Hz and designate them low- and high-frequency bands. Estimates of arrival angle are made in each band as a function of time by cross-correlating band-pass filtered segments of the two hydrophone signals (1.36 and 0.34 s long, respectively, for the low- and high-frequency bands) to determine the delay in arrival time of signal between hydrophones. Let the arrival time delay be the time of the cross-correlation peak measured in units of signal samples and given by n_d, then the signal arrival angle relative to the array axis is given by

$$\theta = \cos^{-1}\left(\frac{\tau_d c}{L}\right), \qquad (1)$$

where the speed of sound is c, the signal is sampled at a rate f_s, and $\tau_d = n_d/f_s$. A single arrival angle was determined for each segment of data processed by picking the time delay of the peak of the cross-correlation function between the two hydrophones.

The theory underlying the beam forming response of this simple two-element array is discussed in the appendix of Deane (1999). Figure 2 shows a theoretical calculation of the broad-band, beam forming response of the array for the two spectral bands chosen, for plane waves arriving broadside to the array and at an angle of 45°. Beam width is greatest for the low-frequency band, and increases as the plane wave arrival angle varies from broadside to end fire. The beam width of the array defines its ability to discriminate between plane waves arriving at different angles. If, however, a source generates a stable arrival, the distribution of angles associated with that source, estimated over time, may be narrower than the array beam width and this is the case for the rose plots of arrival angle presented later.

The angle of arrival relative to the array axis actually describes the angle of a cone along which an incoming wave has propagated, leading to a broadside ambiguity to the angle estimate (see Fig. A1 in Deane, 1999). When the array is oriented to the north, for example, there is no way to tell if a broadside arrival is from the east or west. If the directionality of the noise field is sufficiently stable over time, it is possible to break the array symmetry by rotating the array through 90°. This procedure was adopted with varying levels of success during the deployment. The sources of low-frequency noise were observed to be stable over many minutes (with the exception of ice calving events), and the array ambiguity was resolvable. Noise sources in the high-frequency band were more variable, and it was not always possible to process the ambiguity.

3. Results and concluding remarks

A spectrogram (top) and average power spectral density (bottom, black line) of ambient noise from site 130726/1 is shown in Fig. 3. These data show that noise levels in

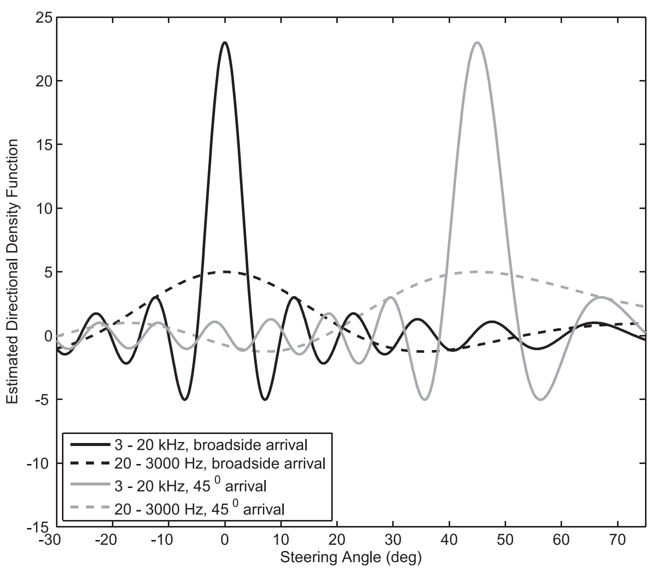

FIG. 2. A plot of the beam forming response of DAB in the two spectral bands and at two different angles of arrival. Details of the theory can be found in the appendix of Deane (1999).

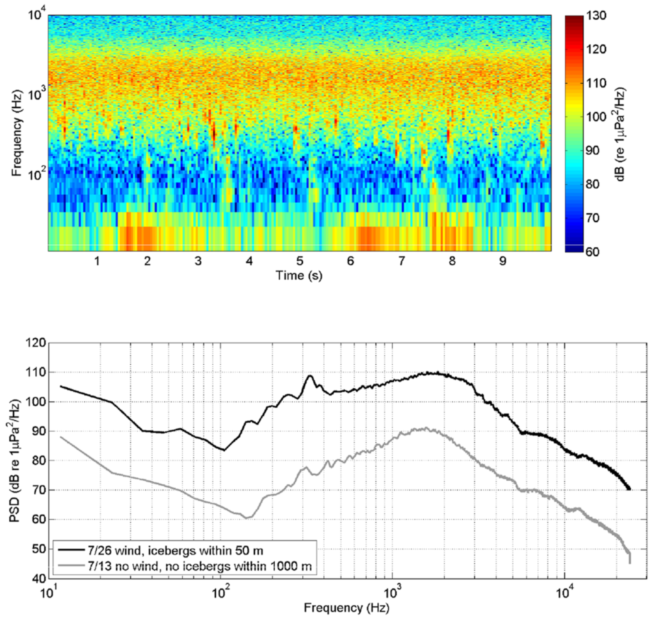

FIG. 3. (Color online) Top: A spectrogram of 10 s of ambient noise measured at site 130726/1 (see Fig. 1). Bottom: Noise power spectral density averaged across the 10 s recording interval.

glacial fjords during the summer months can exceed 100 dB, which is very noisy compared with coastal waters away from glaciers where nominal, maximum noise levels are in the range 70–80 dB at 1 kHz (e.g., Fig. 2, Dahl *et al.,* 2007). Overall noise level in the bay was variable, depending on the mass of ice melting in the bay and conditions of wind and rain, as illustrated by the gray line in the bottom plot taken from 130713/3 during a time with little floating ice and low wind and waves.

It is evident from the spectrogram that noise below 1 kHz tends to be more variable than at higher frequencies. Wind and waves (but not rain) were present on the day of observation and sea state was estimated to be 2–3 in the Beaufort scale. Visual observation of ice-wave interactions from the boat done simultaneously with listening to the hydrophone signal lead to the conclusion that the pulses of sound occurring at a rate of a few per second between 100–500 Hz were due to the lapping of water wave crests on the underside of the periphery of icebergs, which tended to melt preferentially in the water, leaving ice ledges just above the water line.

Results for data collected on July 24th are shown in Fig. 4 as rose plots of arrival angle. The left and right columns, respectively, correspond to the low- and high-frequency bands. The rows correspond to sites 1 (top), 2 (middle), and 3 (bottom), located on Fig. 1. Each wedge in a rose plot shows the percentage of arrivals at the corresponding angle. The color within a wedge designates the proportion of arrivals having a specified amplitude (see legends), with lighter colors corresponding to more intense arrivals. The numerical values correspond to dB re 1 μPa^2 integrated across the indicated frequency band.

Site 1 was located at the mouth of the bay and, on this day a cruise ship passed to the southwest. Both frequency bands at site 1 are dominated by noise from the cruise ship and show a similar pattern of arrivals pointing toward it. This source of opportunity serves as a good indication of the angular accuracy and consistency achieved in both frequency bands. In contrast, sites 2 and 3 are located close to the glacier terminus and the ship had moved out of acoustic range at the time of measurement. Both sites show quite distinct patterns of arrivals in the low- and high-frequency bands, suggesting that different noise production mechanisms are operating

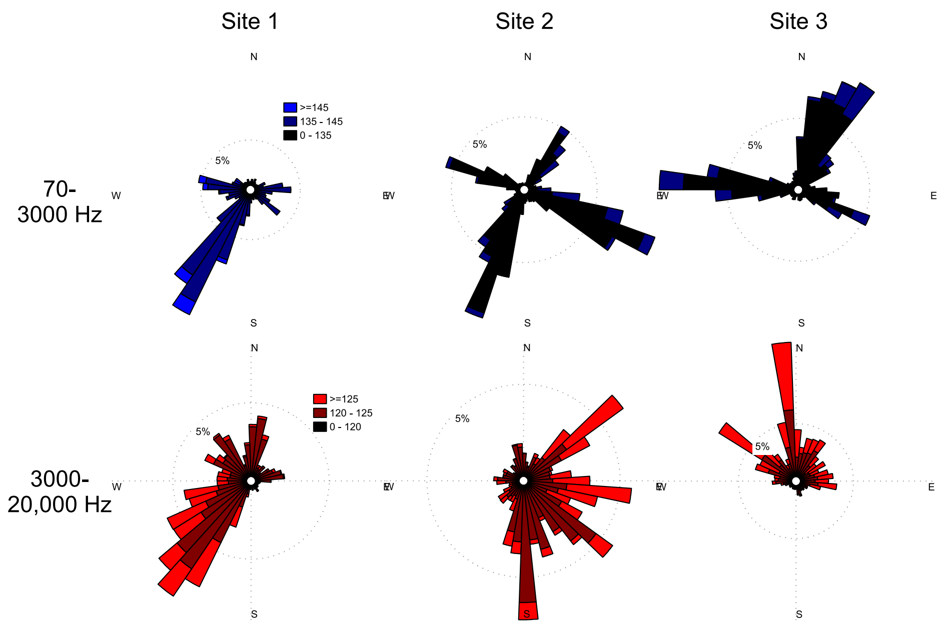

FIG. 4. (Color online) Rose plots of arrival angle as a function of frequency band (columns) and recording site (rows). Each wedge shows the percentage of arrivals falling in the designated angle. Color within a wedge shows the fraction of arrivals within a specified intensity range. Arrival intensity is in dB re 1 μPa^2, and corresponds to power spectral density integrated across the designated frequency band.

within these bands. Both sites 2 and 3 show arrivals from the glacier front in the high-frequency band, with the additional arrival angles at site 2 almost certainly due to a cluster of icebergs scattered around the recording site.

Measurements of ambient noise in the vicinity of tidewater glaciers show promise in providing information about noise source mechanisms and glacier dynamics. The first challenge in using noise to monitor glacier activity is to develop a quantitative link between noise production mechanisms, the spectral bands over which they radiate and their distributions in space and time. The measurements of horizontal directionality presented here demonstrate the increased value of deploying a portable two-hydrophone system over omni-directional measurements and also show that different physical mechanisms do, indeed, radiate noise in distinct spectral bands.

In order to make further progress, multi-hydrophone noise measurements need to be made simultaneously with radar or stereo-photogrammetric measurements of ice distribution in the fjord and calving events from the glacier wall. The significant levels of wave-ice interaction noise in the band 100–500 Hz observed during windy conditions suggests that meteorological and surface wave conditions should be recorded during periods of noise observation. Finally, propagation effects in the complex fjord environment need to be accounted for, along with the development of heuristic and/or quantitative theoretical models of the noise emission from relevant physical processes, such as ice melting and calving events.

Acknowledgments

We gratefully acknowledge the support of the staff at the Polish Polar Research Station in Hornsund, operated by the Institute of Geophysics, Department of Polar and Marine Research, Polish Academy of Sciences. The rose plots were made using a modified version of wind_rose.m by P. Remo, http://www.mathworks.com/matlabcentral/fileexchange/17748-wind-rose. This work has been supported by the Office of Naval Research, Ocean Acoustics Division, Grant No. N00014-1410213, Polish National Science Center Grant

No. 2011/03/B/ST10/04275, and the statutory activity of the Institute of Geophysics Polish Academy of Sciences.

References and links

Carey, M. C., and Evans, R. B. (**2011**). *Ocean Ambient Noise Measurement and Theory. Monograph Series in Underwater Acoustics* (Springer, New York).

Dahl, P. H., Miller, J. H., Cato, D. H., and Andrew, R. K. (**2007**). "Underwater ambient noise," Acoust. Today **3**(1), 23–33.

Deane, G. B. (**1999**). "Acoustic hot spots and breaking wave noise in the surf zone," J. Acoust. Soc. Am. **105**(6), 3151–3167.

Greene, C. R., and Buck, B. B. (**1964**). "Arctic ocean ambient noise," J. Acoust. Soc. Am. **36**(6), 1218–1220.

Keogh, M., and Blondel, P. (**2008**). "Passive acoustic monitoring of ocean weather patterns," in *Proceedings of the Institute of Acoustics*, Vol. 30, Pt. 5.

Macpherson, J. D. (**1962**)."Some under-ice ambient noise measurements," J. Acoust. Soc. Am. **34**(8), 1149–1150.

Milne, A. R., and Ganton, J. H. (**1964**). "Ambient noise under Arctic sea ice," J. Acoust. Soc. Am. **36**(5), 855–863.

Pettit, E. C., Nystuen, J. A., and O'Neel, S. (**2012**). "Listening to glaciers: Passive hydroacoustics near marine-terminating glaciers." Oceanography **25**(3), 104–105.

Scholander, P. F., and Nott, D. C. (**1960**). "Bubble pressures in Greenland icebergs," J. Glaciol. **3**(28), 671–678.

Tegowski, J., Deane, G. B., Lisimenka, A., and Blondel, P. (**2011**). "Detecting and analyzing underwater ambient noise of glaciers on Svalbard as indicator of dynamic processes in the Arctic." in *Proceedings of 4th International Conference and Exhibition on Underwater Acoustic Measurements: Technologies & Results*, Kos Island, Greece (June 20–24, 2011), pp. 1149–1154.

Tegowski, J., Deane, G. B., Lisimenka, A., and Blondel, P. (**2012**). "Spectral and statistical analyses of ambient noise in Spitsbergen Fjords and identification of glacier calving events," in *11th European Conference on Underwater Acoustics 2012, ECUA 2012. Proceedings of the Institute of Acoustics*, St. Albans, pp. 1667–1672.

Urick, R. J. (**1971**). "The noise of melting icebergs," J. Acoust. Soc. Am. **50**(1), 337–341.